# Reliability of Residual Tumor Estimation Based on Navigation Log

Hiroyuki YAMADA,[1] Takashi MARUYAMA,[1,2] Yoshiyuki KONISHI,[1]
Ken MASAMUNE,[1] and Yoshihiro MURAGAKI[1,2]

[1]Faculty of Advanced Techno-Surgery, Tokyo Women's Medical University, Tokyo, Japan
[2]Department of Neurosurgery, Tokyo Women's Medical University, Tokyo, Japan

## Abstract

The mass of residual tumors has previously been estimated using time-series records of the position of surgical instruments acquired from neurosurgical navigation systems (navigation log). This method has been shown to be useful for rapid evaluation of residual tumors during resection. However, quantitative analysis of the method's reliability has not been sufficiently reported. The effect of poor log coverage is dominant in previous studies, in that it did not highlight other disturbance factors, such as intraoperative brain shift. We analyzed 25 patients with a high log-acquisition rate that was calculated by dividing the log-available time by the instrument-use time. We estimated the region of resection using the trajectory of surgical instrument that was extracted from the navigation log. We then calculated the residual tumor region and measured its volume as log-estimation residual tumor volume (RTV). We evaluated the correlation between the log-estimation RTV and the RTV in the post-resection magnetic resonance (MR) image. We also evaluated the accuracy of detecting the residual tumor mass using the estimated residual tumor region. The log-estimation RTV and the RTV in the post-resection MR image were significantly correlated (correlation coefficient = 0.960; $P < 0.001$). The presence of patient-wise residual tumor mass was detected with a sensitivity of 81.8% and a specificity of 92.9%. The individual residual tumor mass was detected with a positive predictive value of 72%. Estimation of residual tumor with adequate log coverage appears to be a suitable method with a high reliability. This method can support rapid decision-making during resection.

Keywords: glioma, intraoperative MRI, log, navigation, residual tumor

## Introduction

Gliomas are invasive malignant brain tumors, the boundaries of which are unclear and difficult to discern with the naked eye. While surgical images, such as magnetic resonance (MR) images, are used to identify tumor regions, they often invade tissues beyond the boundaries that can be recognized using imaging techniques; thus, there is a high probability of recurrence after removal. Microsurgical resection is one of the primary options in the treatment of glioma, and chemotherapy and radiation therapy are also used in combination. The contribution of the extent of resection (EOR) assessed using radiological images to a good treatment outcome is controversial.

However, recent evidence suggests that extensive resection results in a good prognosis.[1–7]

Using neurosurgical navigation to identify the tumor position using MR images has been a popular choice for improving the tumor resection procedure. However, if the navigation system uses MR images obtained from preoperative MR imaging (MRI), the effect of navigation is often suppressed by changes in the tumor position due to brain deformation (brain shift) during surgery. For this reason, intraoperative MRI (iMRI) was introduced to provide intraoperative image updates to compensate for the brain shift.[8–10] Evidence suggests that the combined use of iMRI and navigation can improve removal.[11–13]

Moreover, previous studies have reported that the time-series records of the tip position of the navigation target device (hereafter "navigation log") can be used to intraoperatively grasp the region of resection (ROR) and the residual tumor.[14–16] The term "log" refers to a time-series record of events in computer science. The navigation system superimposes the tip

position of the navigation target device, typically the dedicated navigation probe, on the MR images to show whether the specified point is located in the tumor region. However, it is difficult to understand the three-dimensional (3D) structure of the ROR by manually checking "point-in-space" data. The navigation system, on the contrary, continuously measures the tip position of the target device. By collecting the measured position data from the navigation system and recording them as a time series, the continuous history of "point-in-space" data can be obtained in the form of a navigation log. Furthermore, by registering the surgical instrument (for example, bipolar forceps) as the navigation target device instead of the probe, the history of the resection can also be obtained as part of the navigation log. Reportedly, the 3D structure of the cumulative trajectory that is derived from the navigation log strongly corresponds to that of the actual ROR.[15] Based on this, the intraoperative 3D visualization of the ROR and residual tumor using navigation log was proposed.[14,16] In 50% (3 of 6) of the clinical cases, the residual tumor was detected using the 3D visualization results after the surgeon had obtained the navigation-probe-based ROR confirmation and resection had been performed, as intended.[16] As log-based residual tumor detection does not require an additional time-consuming MRI scan, it could reduce the total surgery time compared to residual tumor detection with iMRI. Furthermore, when preoperative MRI-based navigation is the only available choice, the navigation log can be used for residual tumor detection as a substitute for iMRI.[16]

However, a quantitative analysis of the reliability of the log-based estimation method is not sufficient. A previous study reported several cases where the method was applied successfully, but also reported cases with erroneous volume estimation; the volume may be erroneously estimated due to the poor coverage of log acquisition.[14] However, such erroneous estimation is avoidable. In an optical tracking-based navigation system, a significant problem that prevents the successful log acquisition is the line-of-sight problem; the navigation system fails to track the target device when there are obstacles between the optical sensor and the device. By manually adjusting the position of the optical sensor such that it follows the device and by reducing unnecessary temporal obstacles, this problem can be avoided and the coverage of log acquisition can be improved. Therefore, while evaluating the potential reliability of the log-based method, the effect of insufficient log coverage may be excluded. However, other error-causing factors, including brain shift during resection, may be present and may persist even if the navigation log is collected perfectly. These factors are difficult to avoid and can affect the reliability of log-based estimation. The reliability of log-based estimation under the influence of these factors still seems to be high as long as the log coverage is sufficient, because the results of previous studies,[14–16] which should also have been affected by these factors, indicated good efficacy of this method. However, adequate quantitative analysis of the reliability of log-based estimation in such conditions has not been conducted to date.

Therefore, this study aimed to verify the reliability of residual tumor estimation using a navigation log in situations that excluded only the effect of insufficient log acquisition among various other error-causing factors and aimed to provide statistical support for using log-based estimation methods in intraoperative decision-making. We investigated the accuracy of residual tumor mass detection for patients with high navigation log coverage, as well as the correlation between the estimated residual tumor volume (RTV) and the RTV measured from MR images.

## Materials and Methods

The study design was approved by the Institutional Ethics Review Board at the Tokyo Women's Medical University (No. 4482). The requirement for informed consent of the participants was waived.

### Participants

Between January 2015 and July 2016, 73 consecutive adult patients who had been diagnosed with glioma and had undergone resection with navigation log recording in a single facility were included in this retrospective study as potentially eligible patients. Patients having insufficient data for analysis or those whose log acquisition rate (estimated by the method discussed below) was lower than the threshold (80%) were excluded from the study.

### Data collection

The intraoperative MR images were obtained using the 0.4-T MRI system APERTO (Hitachi, Chiyoda, Tokyo, Japan). The first MRI scan was performed before resection, and the second scan was performed according to the surgeon's decision during resection. Additional MRI scans were performed during resection if required by the surgeon, and the final MRI scan was performed after resection. In this study, the difference between the MR image obtained from the first MRI and the MR image obtained from the second MRI was analyzed.

During resection, the navigation log was collected from a commercially available navigation system, Curve (Brainlab AG, Munich, Germany). The bipolar forceps were set as the navigation target device.

Since the navigation system itself did not have the functionality for recording the navigation log, we created an application to record the log in the laboratory. The navigation system was equipped with a data output interface using OpenIGTLink (http://openigtlink.org), the open standard network protocol proposed by Tokuda et al. for obtaining navigation information.[17] During resection, our application continuously acquired the measured device position data series (position of the device tip and angle of the device) from the navigation system via the OpenIGTLink protocol and recorded the data of each position with its acquisition timestamp as one navigation log record. The navigation log was collected at a maximum rate of 20 records per second.

A microscopic movie was recorded during the resection. The resolution was 1920 × 1080, and the frame rate was 29.97 frames per second.

### Estimation of the log acquisition rate

The log acquisition rate was calculated using the following formula: the time at which the navigation target device was used and the navigation log was successfully collected/the time at which the navigation target device was used.

The log acquisition rate for each patient was estimated by analyzing the microscopic movie using the application created by us and our colleague in the laboratory. Given that the navigation target device (bipolar forceps) used in the facility was blue colored, the time at which the corresponding frame images of the microscopic movie contained enough blue pixels (10,000 pixels) was estimated as the device-used time. The time at which the above blue-pixel criteria was satisfied and enough navigation log records (5 records/sec) were recorded was estimated as the log-available time. The log-acquisition rate was estimated by dividing the log-available time by the device-used time.

### Segmentation and tumor model construction

Tumor segmentation was performed on the first and second MR images, and a 3D tumor model was constructed using the segmentation results. A pre-resection tumor model was constructed from the tumor region of the first MR image (the pre-resection tumor region), and its volume was calculated as the pre-resection tumor volume. An image-based residual tumor model was constructed from the tumor region of the second MR image (the image-based residual tumor region) and its volume was calculated as image-based RTV. Since several volumetric studies have used segmentation for measuring tumor volume, we used the image-based residual tumor model as a reference standard for residual tumor evaluation.

For Grade IV glioma patients, segmentation was performed on the T1-contrasted lesion. For other patients, segmentation was performed for the T2 high-signal lesion and the T1 low-signal lesion. Segmentation results were checked by an expert radiologist and an expert neurosurgeon who were unaware of the log-based estimation results discussed in the following. For segmentation and 3D model construction, 3D Slicer (http://www.slicer.org), an open source software, was used.

### Residual tumor estimation

The ROR was estimated using the navigation log. The trajectory of the device tip and the speed of movement were analyzed using the navigation log. The brain region of the first MR image through which the device tip passed at a speed lower than the threshold (30 mm/sec) was considered the "resection-revealed region." The brain region that was enclosed by the resection-revealed region and the surface of brain was considered the "enclosed region." The brain surface was used as the part of the enclosure since the resection process often hollowed out the tumor region by resecting only the tumor boundary in the brain region. The resection-revealed region and the enclosed region were combined as the ROR estimated using navigation log (log-estimation ROR).

The log-estimation residual tumor region was estimated by subtracting the log-estimation ROR from the pre-resection tumor region. The log-estimation residual tumor model was constructed from the log-estimation residual tumor region, and its volume was measured as log-estimation RTV.

To check the existence of residual tumor sections of a sufficiently large size, residual tumor sections that were larger than a 6-mm-sized cube were extracted as "residual tumor masses." The log-estimation residual tumor masses were extracted from the log-estimation residual tumor region, and the image-based residual tumor masses were extracted from the image-based residual tumor region. Each patient could have multiple residual tumor masses separated by the ROR even if the pre-resection tumor region was not multifocal.

For processing these estimations and model constructions, the 3D space of the first MR image was divided into 2-mm-sized cubes (grid cubes), and the grid cubes were used as minimum units for these processes. Grid cubes through which the device tip passed at a speed lower than the threshold (30 mm/sec) were extracted as "device-passage cubes." The device-passage cubes located in the brain region were extracted as "resection-revealed cubes." Grid cubes enclosed by the resection-revealed

cubes and the surface of brain were extracted as "enclosed cubes." In extracting the enclosed cubes, cracks with a width of one grid cube in the resection-revealed cube enclosure were interpolated. The resection-revealed cubes and the enclosed cubes were then combined as "log-estimation ROR cubes." The pre-resection tumor model was constructed by subtracting the log-estimation ROR cubes from the pre-resection tumor model. Residual tumor sections that contained a 6 mm-sized cube (27 [3 × 3 × 3] pieces of grid cubes) were extracted as the residual tumor mass. This processing was performed by the application created by us using the Visualization Toolkit (http://www.vtk.org) library.

### Visualization for the resection process analysis

To visualize the resection process, the resection time was divided into resection stages with equal time length and part of the brain region that was the target of resection at each resection stage was superimposed on the slices of the first MR image with a resection-stage-specific color. Grid cubes through which the device tip passed at a speed lower than the threshold (5 mm/sec) was extracted as "resection-work cubes." Each resection-work cube was superimposed on the MR image slice with the color specific to the resection stage in which the device tip first passed through the cube. The resection-stage-specific colors from the beginning to the end of resection were gradually arranged in a rainbow color order (from blue, through green and yellow, to red).

Visualization was performed by the application created by us in the laboratory and 3D Slicer. Our application extracted the resection-work cubes and created the complete data set that could be opened by the 3D Slicer and was ready for the superimposed view. The 3D Slicer was simply used as viewer application.

### Statistical methods

The correlation between log-estimation RTV and image-based RTV was evaluated. Sensitivity, specificity, positive predictive value (PPV), and negative predictive value (NPV) with a 95% confidence interval (CI) for detecting patient-wise residual tumor mass were investigated by checking whether the patients who had log-estimation residual tumor masses also had image-based residual tumor masses, and vice versa. Furthermore, PPV for detecting individual residual tumor mass was investigated by checking whether, for each log-estimation residual tumor mass, an image-based residual tumor mass existed in the location that anatomically corresponded to the location of the log-estimation residual tumor mass. The PPV for detecting any individual residual

tumor sections was also examined by checking whether, for each log-estimation residual tumor mass, any sections of the image-based residual tumor model that could be smaller than a 6 mm-sized cube existed in the corresponding anatomical location. The JMP Pro version 11.2.0 software (SAS Institute, Cary, NC, USA) was used for analysis. The level of statistical significance was set at $P = 0.05$.

### Processing time measurement

Processing times for estimating the residual tumor and visualizing the resection process were measured for each patient. For residual tumor estimation, the time to calculate the log-estimation RTV using the pre-resection residual tumor model was measured. For visualization of the resection process, the time for creating the visualization data set was measured. The measurement for each patient was performed in the same environment (dual-core Core i7 2.4 GHz processor with 16 GB memories).

## Results

### Participants

Seventy-three consecutive adult patients were included in the initial patient population, and 25 patients were selected for analysis. Fifteen patients with insufficient data were excluded (2 patients for insufficient navigation log, 8 patients for insufficient microscope movie, and 5 patients for insufficient MR images). An additional 33 patients with a log-acquisition rate lower than 80% were excluded. The mean patient age was 40.8 years (standard deviation [SD] 10.5 years). The number of male and female patients were 13 and 12, respectively. The number of patients with the main tumor region located in the frontal lobe, temporal lobe, parietal lobe, and insula were 14, 5, 3, and 3, respectively. The number of patients with Grades I, II, III, and IV gliomas were 1, 11, 9, and 4, respectively. The median and mean values of the estimated log-acquisition rate were 87.5% (range 80.5%–97.8%) and 88.8% (SD 5.1%), respectively. The median and mean pre-resection tumor volumes were 33.6 cm³ (range 2.5–116.7 cm³) and 41.7 cm³ (SD 31.6 cm³), respectively. The median and mean image-based RTVs were 5.0 cm³ (range 0.0–52.3 cm³) and 9.6 cm³ (SD 12.3 cm³), respectively. The median and mean log-estimation RTVs were 3.1 cm³ (range 0.03–44.8 cm³) and 9.6 cm³ (SD 12.1 cm³), respectively. The median and mean values of the EOR were 81.2% (range 36.1%–100.0%) and 78.4% (SD 17.7%), respectively, where EOR was calculated as follows: (pre-resection tumor volume − image-based RTV)/ (pre-resection tumor volume).

## Volume correlation

Figure 1 shows the result of volume correlation analysis between log-estimation RTV and image-based RTV. Pearson's correlation coefficient was 0.960 ($P <0.001$). The coefficient of the regression line was $0.972x + 0.276$ ($R^2$ 0.92, root mean square error 3.540).

## Accuracy of patient-wise residual tumor detection

Table 1 summarizes the result of accuracy analysis of detecting patient-wise residual tumor existence. Sensitivity and specificity of the log-based residual tumor detection were 81.8% (95% CI: 52.3%, 94.9%) and 92.9% (95% CI: 68.5%, 98.7%), respectively. The PPV and the NPV were 90.0% (95% CI: 59.6%, 98.2%) and 86.7% (95% CI: 62.1%, 96.3%), respectively.

## Accuracy of individual residual tumor mass detection

Twenty-five pieces of log-estimation residual tumor masses were extracted from 10 patients. The image-based residual tumor mass provided 18 pieces, the corresponding sections of residual tumor that were smaller than a 6 mm-sized cube provided 5 pieces, while no corresponding residual tumor existed for the remaining 2 pieces. The PPV was 72% and 92% for detecting the individual residual tumor mass and for detecting any individual residual tumor sections, respectively.

## Processing time measurement

The mean processing times of residual tumor estimation for 25 patients and that of resection process visualization were 18.9 sec (SD 10.8 sec) and 3.7 sec (SD 1.9 sec), respectively. The maximal processing times for residual tumor estimation and resection process visualization were 38.8 and 8.5 sec, respectively.

## Illustrative cases

Figure 2 illustrates the process of residual tumor estimation. We estimated and constructed the log-estimation residual tumor model from the pre-resection tumor model and the navigation log (Figs. 2A–2C and 2E–2G). We also constructed an image-based residual tumor model (Figs. 2D and 2H) for reference standard. In the case of Fig. 2, the log-estimation RTV and the image-based RTV were 5.7 cm³ and 4.9 cm³, respectively. One log-estimation residual tumor mass was detected, for which the corresponding image-based residual tumor mass existed. The log-acquisition rate was estimated to be 86.14%.

Figure 3 illustrates the visualization for resection process analysis for 2 patients. Four panels illustrate each patient's visualization. The first two panels show the result of the resection process visualization,
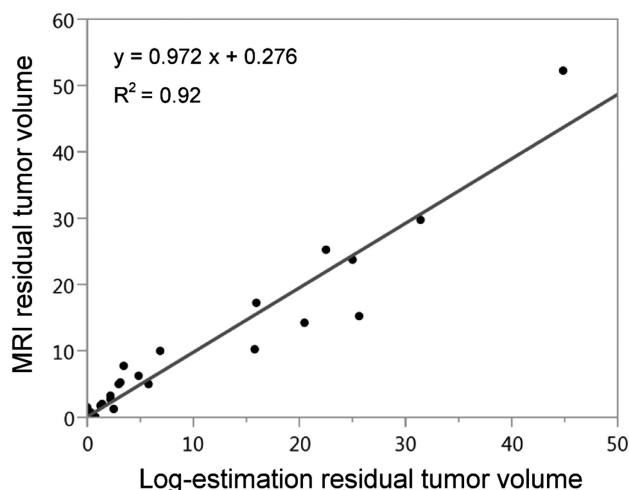


Fig. 1 **Correlation between log-estimation RTV and image-based RTV. RTV: residual tumor volume**

and the remaining two panels show the result of the residual tumor analysis on the corresponding slice. For the first patient, the log-estimation RTV and image-based RTV were 31.4 cm³ and 29.7 cm³, respectively. Six log-estimation residual tumor masses were detected, and in five of these, corresponding image-based residual tumor masses were present. In the remaining one, no corresponding residual tumor could be confirmed. The log-acquisition rate was estimated to be 93.49%. For the second patient, the log-estimation RTV and image-based RTV were 15.8 cm³ and 10.2 cm³, respectively. One log-estimation residual tumor mass was detected, and the corresponding residual tumor could not be confirmed. The log-acquisition rate was estimated to be 86.40%.

After the analysis period of this study, resection process visualization was used to detect the residual tumor during actual resection. Figure 4 illustrates a case of intraoperative use during resection. Figures 4A and 4B show the distribution of the resection-work cubes used to confirm the presence of the residual tumor in the middle stage of the resection. Figures 4C and 4D show the final distribution of the resection-work cubes, indicating that additional resection was performed in the region considered a residual tumor.

## Discussion

This study has demonstrated that if the coverage of the navigation log was sufficiently high, the estimated RTV was significantly correlated with the iMRI-based RTV. The processing of residual tumor estimation required only a short time and could be repeated as many times as required. It was suggested

**Table 1  Contingency table of residual tumor detection for patients**

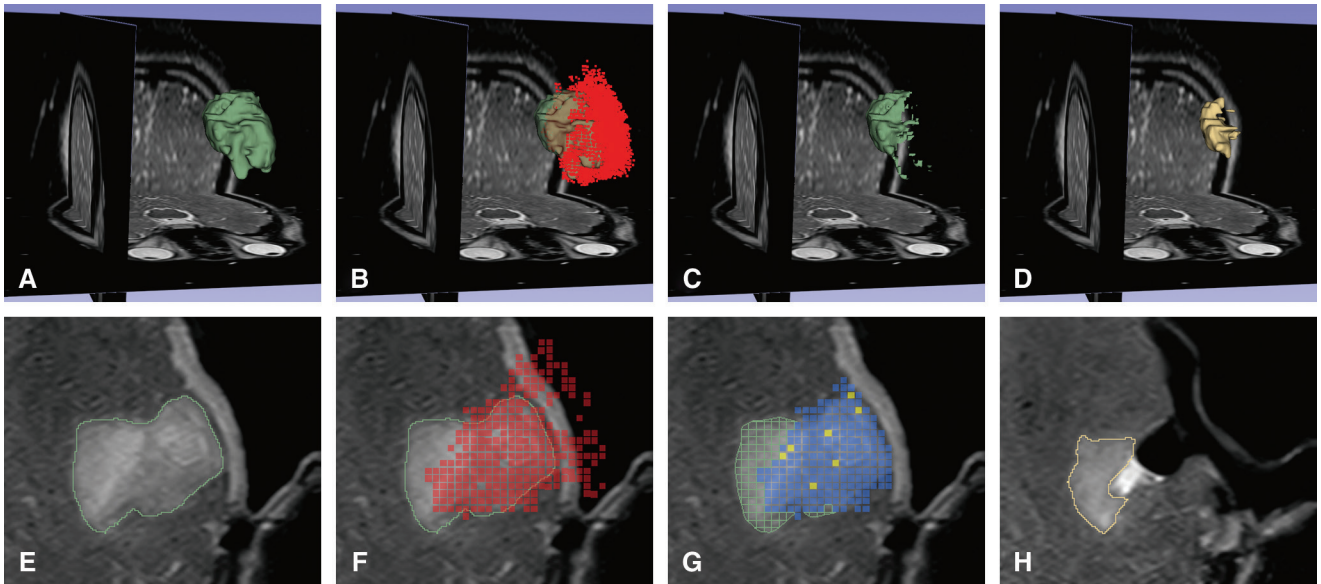|  |  | MRI | | Total |
|---|---|---|---|---|
|  |  | Positive | Negative |  |
| Log-estimation | Positive | 9 | 1 | 10 |
|  | Negative | 2 | 13 | 15 |
| Total |  | 11 | 14 | 25 |

MRI: magnetic resonance imaging



**Fig. 2  Illustration of residual tumor analysis. (A)–(C) and (E)–(G) illustrate the estimation and construction of the log-estimation residual tumor model and (D) and (H) illustrate the construction of the corresponding image-based residual tumor model. (A) shows the pre-resection tumor model constructed from the segmentation result of the first MR image (E). (B) and (F) illustrate the extraction of device-passage cubes (red-colored cubes and squares). (C) shows the log-estimation residual tumor model constructed based on the estimation result in (G), where the resection-revealed cubes (blue-colored squares) and the enclosed cubes (yellow-colored squares) are extracted and the remaining tumor region is extracted as the log-estimation residual tumor region (green-colored frame). (D) shows the image-based residual tumor model constructed from the segmentation result of the second MR image (H). MR: magnetic resonance**

that the log-based estimation method enabled reliable and rapidly repeatable intraoperative RTV estimation and monitoring.

The evaluation of log-estimation reliability in this study could provide statistical support for using log-based estimation methods in intraoperative decision-making. Recent studies[1–3,5–7] have suggested that even when total removal cannot be expected, a better prognosis can be obtained with a higher EOR. Therefore, the log-based estimation of RTV and EOR can help rapidly decide whether the resection should be continued when total removal is difficult. Furthermore, a series of studies reported that the prognosis of partial resection followed by chemotherapy varied

depending on the subtype of low-grade glioma[5] and proposed a resection strategy that assigned a different EOR target to low-grade eloquent glioma, depending on its genetic classification, which was identified by intraoperative molecular diagnosis.[18] The preoperative prediction of the genetic classification using deep learning would be combined in future.[19] The log-based estimation could support execution of such resection strategies by providing intraoperative EOR monitoring.

The results of this study also showed that the existence of the residual tumor mass could be detected with a high sensitivity and specificity using the log-based method. The individual residual tumor
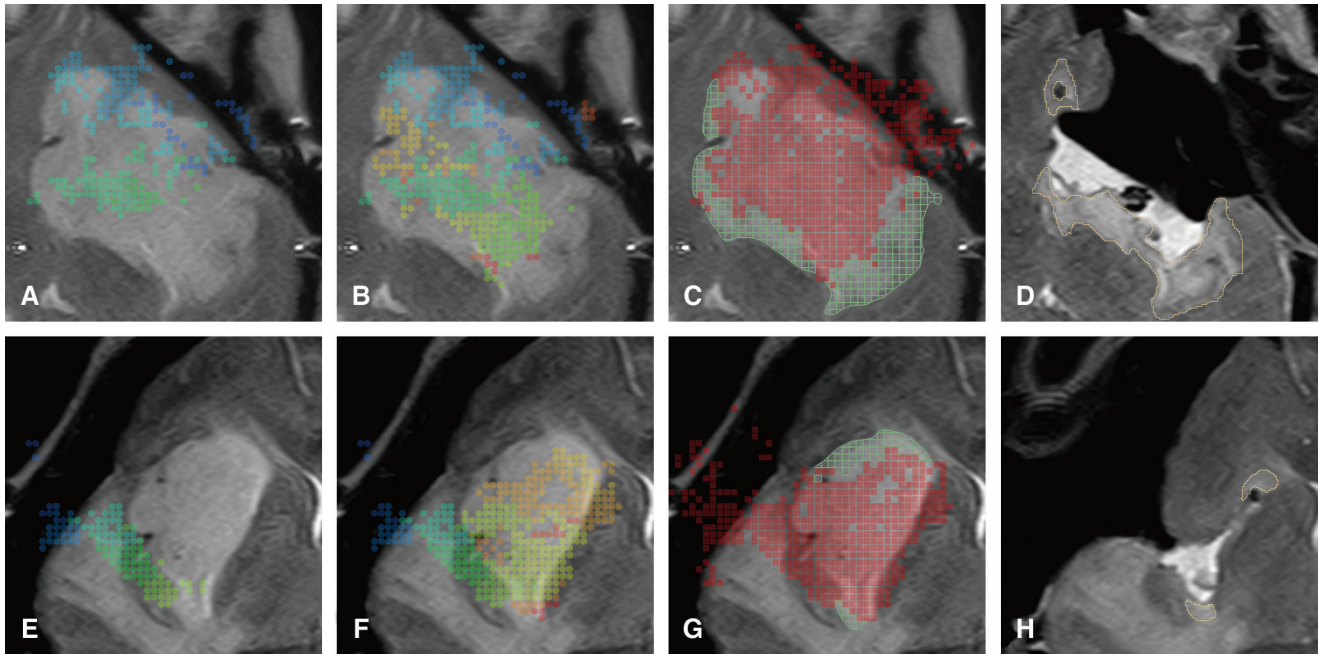
**Fig. 3  Resection process visualization. This figure illustrates visualizations for two patients; (A)–(D) are for the first patient and (E)–(H) are for the second patient. For each patient, the first two panels show the migration of current-resection region; the first and second panels show the distribution of the resection-work cubes in the first half and the whole of the resection time, respectively. The color of resection-work cubes for each resection stage is gradually shifted in a rainbow color order (from blue, through green and yellow, to red). The third panel shows the final distribution of the corresponding device-passage cubes (red-colored squares) and log-estimation residual tumor region (green-colored frame) on the same slice. The fourth panel shows image-based residual tumor region (yellow-colored frame) on the corresponding slice in the second MR image. MR: magnetic resonance**

detection also demonstrated a high PPV. It was suggested that log-based residual tumor mass detection could support the decision of additional resection.

To the best of our knowledge, this is the first study that validated the reliability of the log-based RTV estimation by quantitative analysis. A previous study with 5 clinical cases reported erroneous estimation results in large percentage of their cases and guessed that log-coverage problem would cause the estimation error.[14] Another study using preoperative MRI with 17 cases validated the effectiveness of log-based residual tumor estimation but abandoned log-based EOR estimation.[15]

This study proposed the new log-based method for EOR evaluation. The previous study proposed the estimation method that considered points between the central point of tumor and the valid log point as interior of the resected tumor region.[14] Such a method cannot accurately estimate the tumor region having a concave shape as well as the tumor region hollowed out together with the brain surface. Our method does not have such limitations.

Resection process visualization can be used to understand how resection was performed. Figure 3 depicts the transition of the visualization result in

the same patient and the differences in the resection process between the two patients. Such visualization results can help surgeons identify the current resection state. The results can also be used to analyze the side effects of resection, such as brain shift, as discussed later.

The visualization result can be used for residual tumor detection as well. Although our visualization result could not provide automatic residual tumor detection and volume evaluation, the residual tumor mass could be identified, as illustrated in Figure 4. Since the visualization process does not require a pre-resection tumor model, it can be used as an alternative when intraoperative segmentation is difficult.

The visualization result could also be used for evaluating the efficiency and appropriateness of the resection process. Each group of the resection-work cubes in the two illustrated cases was compactly crowded in the specific region. Contrarily, when the surgeon did not have the clear resection strategy, the resection-work cubes were scattered in many areas and the final distribution of the resection-work cubes became in disorder. A previous study proposed the method for evaluating the appropriateness of surgery using navigation log.[20] This study proposed
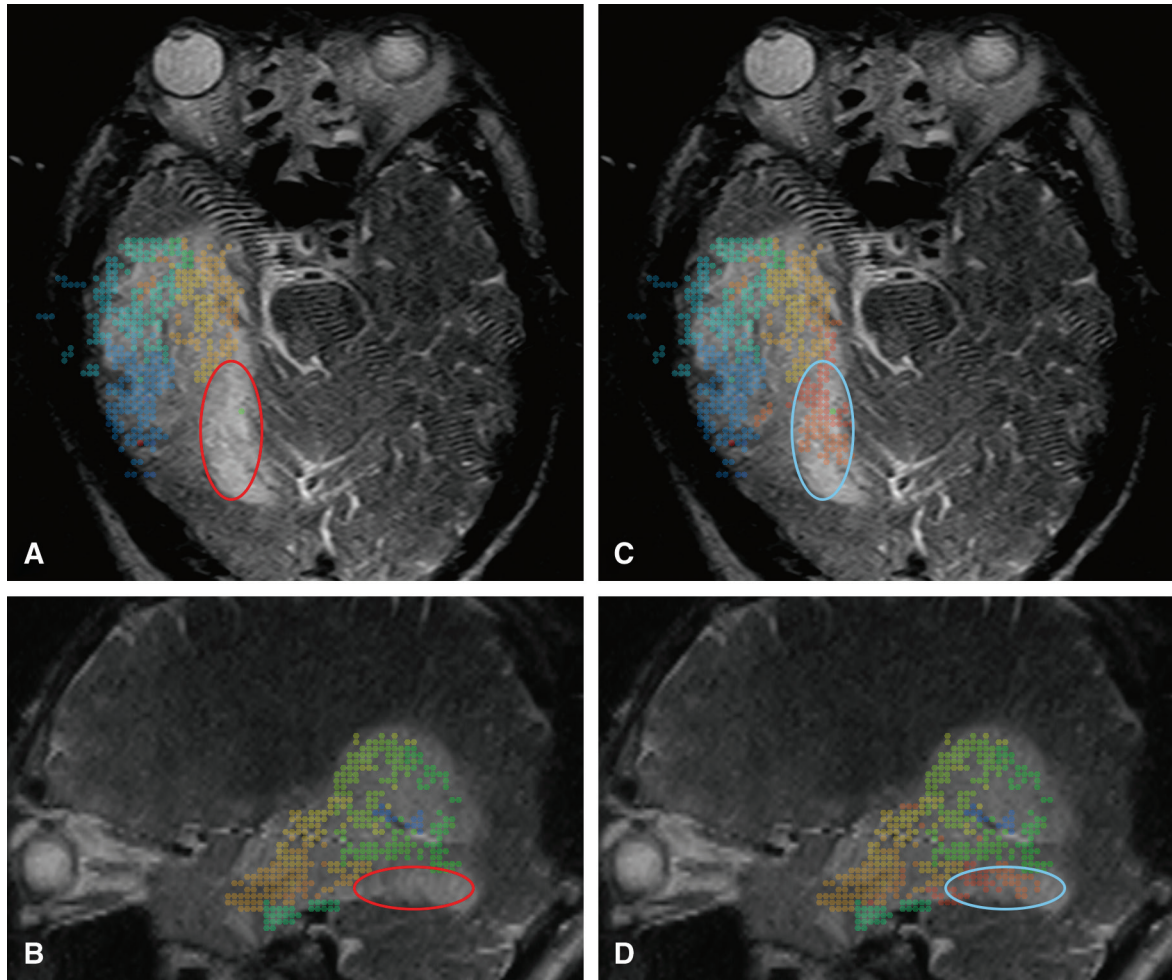
**Fig. 4 Residual tumor identification and additional resection based on the log-based estimation. (A) and (B) show the distribution of resection-work cubes at the residual tumor identification. The tumor region not covered by the resection-work cubes (red-colored ellipse) is identified as the residual tumor region. (C) and (D) show the final distribution of resection-work cubes and the region of additional resection (light-blue-colored ellipse) after residual tumor identification.**

another evaluation method that was intuitive and applicable in actual clinical cases.

This study proposed the new method to visualize the resection process more clearly. The previous study used all the logged points to visualize the resection process.[15] These points could contain the points related to actual resection work and the points related to the movement of the device in the resection cavity. We visualized only the former points using the tip speed criteria with a lower threshold (5 mm/sec).

This study also proposed the method to estimate the coverage of navigation log more rigidly. The previous study estimated the log coverage by dividing the tumor volume by the number of logged points.[14] There is a greater tendency for the number of logged points to increase as the EOR becomes higher.

Therefore, when patients with a high log coverage are selected using that method, there is a strong possibility that the EOR is biased. This study was free from such selection bias.

The result of measuring the processing time showed that both RTV estimation and resection process visualization could be rapidly executed during resection. Both methods were automated by the application program we developed, and each processing action could be executed by a single command. This automation improved the processing time by eliminating the time loss due to manual operation and increasing the accessibility to the methods. As a result, our methods can be easily and rapidly applied at any time during resection.

The brain shift during resection[21–25] is a risk factor for an error in the log-based estimation. Shifting of

the residual tumor to the resection cavity could prevent us from obtaining the trajectory concerning the residual tumor removal; thus, the residual tumor could be overestimated. Further, the shift of residual tumor away from the original tumor region may result in underestimation. In this study, there were cases where a strong brain shift was observed. In the second case of Figure 3, in which the lesion on the lower side of the tumor (in the direction of gravity) was resected first, the tumor volume was overestimated by a large margin (5.6 cm³). As confirmed by the resection process analysis, it is considered that the lower side of the tumor was removed earlier, resulting in a downward brain shift to the resection cavity and an erroneous estimation in the upper part of the tumor. In contrast, in the first case, the upper side was resected at an earlier stage, and the erroneous estimation was suppressed to a relatively low level (1.6 cm³). The resection process analysis could be useful in anticipating the extent of brain shift and might be able to help reduce the estimation error in the future study.

There are several limitations to this study. First, many cases were excluded from this study by the log-acquisition rate criteria. This study intended to clarify the log-based estimation reliability that was not suffered from the effect of the log coverage. Therefore, we had to exclude many cases. In our facility, the area in which the optical sensor could be located was limited; therefore, the line-of-sight problem was unavoidable in several cases and typically depended on the location of the tumor lesion (left side or right side). As a result, although the applicability of log-based estimation is not restricted by the nature of each case, the actual applicability in our facility was affected by the tumor location. To continuously achieve high coverage, it is conceivable to adopt a surgical navigation system using magnetic tracking or a multiple-optical-sensor system. Second, this study used bipolar forceps as the navigation target device. Since actual tumor removal was performed using a suction device, the tip position of the bipolar forceps was merely an approximation of the tumor removal point. Moreover, the suction device was solely used in such cases as those involving cyst removal, and such removal processes could not be mapped from the trajectory of the bipolar forceps. Therefore, in a facility where another device that is directly used for tumor removal (such as CUSA) can be registered as the navigation target device, the resulting reliability of the estimation method might differ. Third, the cases in this study were obtained from a single facility. Since the removal strategy affects the degree of brain shift, the results may be different in other facilities. Research at multiple facilities is necessary to verify our results.

One of the extensions of this study in future would be estimation and compensation of brain shift using navigation log and more accurate and robust log-based residual tumor estimation using such compensation result. Using estimation method proposed in this study, the chronological transition of the estimated resection cavity (3D model of ROR) can be tracked and used for quantitatively estimating the extent of brain shift into the estimated resection cavity.

## Conclusions

In this study, the reliability of the residual tumor estimation method using the navigation log was evaluated for patients who were not affected by the low degree of log acquisition. The estimated RTV was significantly correlated with the RTV measured from the MR image, patient-wise existence detection of residual tumor mass demonstrated a high sensitivity and specificity, and the individual residual tumor mass detection demonstrated a high PPV. This suggests that the log-estimation method of detection can provide a highly reliable and rapidly repeatable evaluation of residual tumors and can support a rapid decision-making process during the surgical resection.

## Conflicts of Interest Disclosure

All authors have no conflict of interest.

## References

1) Fujii Y, Muragaki Y, Maruyama T, et al.: Threshold of the extent of resection for WHO Grade III gliomas: retrospective volumetric analysis of 122 cases using intraoperative MRI. *J Neurosurg* 129: 1–9, 2018

2) Fukui A, Muragaki Y, Saito T, et al.: Volumetric analysis using low-field intraoperative magnetic resonance imaging for 168 newly diagnosed supratentorial glioblastomas: effects of extent of resection and residual tumor volume on survival and recurrence. *World Neurosurg* 98: 73–80, 2017

3) Lacroix M, Abi-Said D, Fourney DR, et al.: A multivariate analysis of 416 patients with glioblastoma multiforme: prognosis, extent of resection, and survival. *J Neurosurg* 95: 190–198, 2001

4) Li YM, Suki D, Hess K, Sawaya R: The influence of maximum safe resection of glioblastoma on survival in 1229 patients: can we do better than gross-total resection? *J Neurosurg* 124: 977–988, 2016

5) Nitta M, Muragaki Y, Maruyama T, et al.: Proposed therapeutic strategy for adult low-grade glioma based on aggressive tumor resection. *Neurosurg Focus* 38: E7, 2015

6) Sanai N, Berger MS: Glioma extent of resection and its impact on patient outcome. *Neurosurgery* 62: 753–764; discussion 264-266, 2008

7) Smith JS, Chang EF, Lamborn KR, et al.: Role of extent of resection in the long-term outcome of low-grade hemispheric gliomas. *J Clin Oncol* 26: 1338–1345, 2008

8) Hata N, Muragaki Y, Inomata T, et al.: Intraoperative tumor segmentation and volume measurement in MRI-guided glioma surgery for tumor resection rate control. *Acad Radiol* 12: 116–122, 2005

9) Iseki H, Nakamura R, Muragaki Y, et al.: Advanced computer-aided intraoperative technologies for information-guided surgical management of gliomas: Tokyo Women's Medical University experience. *Minim Invasive Neurosurg* 51: 285–291, 2008

10) Orringer DA, Golby A, Jolesz F: Neuronavigation in the surgical management of brain tumors: current and future trends. *Expert Rev Med Devices* 9: 491–500, 2012

11) Kubben PL, Scholtes F, Schijns OE, et al.: Intraoperative magnetic resonance imaging versus standard neuronavigation for the neurosurgical treatment of glioblastoma: a randomized controlled trial. *Surg Neurol Int* 5: 70, 2014

12) Muragaki Y, Iseki H, Maruyama T, et al.: Information-guided surgical management of gliomas using low-field-strength intraoperative MRI. *Acta Neurochir Suppl* 109: 67–72, 2011

13) Senft C, Bink A, Franz K, Vatter H, Gasser T, Seifert V: Intraoperative MRI guidance and extent of resection in glioma surgery: a randomised, controlled trial. *Lancet Oncol* 12: 997–1003, 2011

14) Hong J, Muragaki Y, Nakamura R, Hashizume M, Iseki H: A neurosurgical navigation system based on intraoperative tumour remnant estimation. *J Robot Surg* 1: 91–97, 2007

15) Woerdeman PA, Willems PW, Noordmans HJ, van der Sprenkel JW: The analysis of intraoperative neurosurgical instrument movement using a navigation log-file. *Int J Med Robot* 2: 139–145, 2006

16) Woerdeman PA, Willems PWA, Noordmans HJ, Tulleken CAF, van der Sprenkel JWB: The impact of workflow and volumetric feedback on frameless image-guided neurosurgery. *Neurosurgery* 64: 170–175, 2009

17) Tokuda J, Fischer GS, Papademetris X, et al.: OpenIGTLink: an open network protocol for image-guided therapy environment. *Int J Med Robot* 5: 423–434, 2009

18) Koriyama S, Nitta M, Kobayashi T, et al.: A surgical strategy for lower grade gliomas using intraoperative molecular diagnosis. *Brain Tumor Pathol* 35: 159–167, 2018

19) Matsui Y, Maruyama T, Nitta M, et al.: Prediction of lower-grade glioma molecular subtypes using deep learning. *J Neurooncol* 146: 321–327, 2020

20) Sugino T, Kawahira H, Nakamura R: Surgical task analysis of simulated laparoscopic cholecystectomy with a navigation system. *Int J Comput Assist Radiol Surg* 9: 825–836, 2014

21) Gerard IJ, Kersten-Oertel M, Petrecca K, Sirhan D, Hall JA, Collins DL: Brain shift in neuronavigation of brain tumors: a review. *Med Image Anal* 35: 403–420, 2017

22) Nabavi A, Black PM, Gering DT, et al.: Serial intraoperative magnetic resonance imaging of brain shift. *Neurosurgery* 48: 787–797; discussion 797-798, 2001

23) Nimsky C, Ganslandt O, Cerny S, Hastreiter P, Greiner G, Fahlbusch R: Quantification of, visualization of, and compensation for brain shift using intraoperative magnetic resonance imaging. *Neurosurgery* 47: 1070–1079; discussion 1079-1080, 2000

24) Nimsky C, Ganslandt O, Hastreiter P, Fahlbusch R: Intraoperative compensation for brain shift. *Surg Neurol* 56: 357–364; discussion 364-365, 2001

25) Trantakis C, Tittgemeyer M, Schneider JP, et al.: Investigation of time-dependency of intracranial brain shift and its relation to the extent of tumor removal using intra-operative MRI. *Neurol Res* 25: 9–12, 2003

_____

*Address reprint requests to:* Yoshihiro Muragaki, MD, PhD, Faculty of Advanced Techno-Surgery, Tokyo Women's Medical University, 8-1 Kawada-cho, Shinjuku-ku, Tokyo 162-8666, Japan
*e-mail:* ymuragaki@twmu.ac.jp